Evidence for the role of endosymbionts in regional-scale habitat partitioning by hydrothermal vent symbioses

Roxanne A. Beinart[a], Jon G. Sanders[a], Baptiste Faure[b,c], Sean P. Sylva[d], Raymond W. Lee[e], Erin L. Becker[b], Amy Gartman[f], George W. Luther III[f], Jeffrey S. Seewald[d], Charles R. Fisher[b], and Peter R. Girguis[a,1]

[a]Department of Organismic and Evolutionary Biology, Harvard University, Cambridge, MA 02138; [b]Biology Department, Pennsylvania State University, University Park, PA 16802; [c]Institut de Recherche pour le Développement, Laboratoire d'Ecologie Marine, Université de la Réunion, 97715 Saint Denis de La Réunion, France; [d]Department of Marine Chemistry and Geochemistry, Woods Hole Oceanographic Institution, Woods Hole, MA 02543; [e]School of Biological Sciences, Washington State University, Pullman, WA 99164; and [f]School of Marine Science and Policy, University of Delaware, Lewes, DE 19958

Deep-sea hydrothermal vents are populated by dense communities of animals that form symbiotic associations with chemolithoautotrophic bacteria. To date, our understanding of which factors govern the distribution of host/symbiont associations (or holobionts) in nature is limited, although host physiology often is invoked. In general, the role that symbionts play in habitat utilization by vent holobionts has not been thoroughly addressed. Here we present evidence for symbiont-influenced, regional-scale niche partitioning among symbiotic gastropods (genus *Alviniconcha*) in the Lau Basin. We extensively surveyed *Alviniconcha* holobionts from four vent fields using quantitative molecular approaches, coupled to characterization of high-temperature and diffuse vent-fluid composition using gastight samplers and in situ electrochemical analyses, respectively. Phylogenetic analyses exposed cryptic host and symbiont diversity, revealing three distinct host types and three different symbiont phylotypes (one ε-proteobacteria and two γ-proteobacteria) that formed specific associations with one another. Strikingly, we observed that holobionts with ε-proteobacterial symbionts were dominant at the northern fields, whereas holobionts with γ-proteobacterial symbionts were dominant in the southern fields. This pattern of distribution corresponds to differences in the vent geochemistry that result from deep subsurface geological and geothermal processes. We posit that the symbionts, likely through differences in chemolithoautotrophic metabolism, influence niche utilization among these holobionts. The data presented here represent evidence linking symbiont type to habitat partitioning among the chemosynthetic symbioses at hydrothermal vents and illustrate the coupling between subsurface geothermal processes and niche availability.

chemoautotrophy | symbiosis | endosymbiosis

Niche partitioning, the process wherein coexisting organisms occupy distinct niches, is thought to be essential in structuring many biological communities (1–3). Classic studies of ecological niche partitioning have focused on how the intrinsic traits of organisms allow them to occupy or use distinct habitats or resources (4, 5). However, species also can access novel niche space via symbiotic associations with other organisms. In these cases, the niche of the host is expanded through the addition of the symbiont's physiological capabilities. With increasing awareness of the prevalence of microbe–animal associations, the effect of the symbiont(s) on niche utilization may prove to be key to understanding the coexistence of organisms in many biological communities. This effect is likely to be especially important in ecosystems structured by coexisting symbiotic associations, such as hydrothermal vents. Therefore, we looked for habitat-utilization patterns reflective of symbiont-influenced niche partitioning among a group of closely related snail–bacterial symbioses in the Eastern Lau Spreading Center (ELSC) hydrothermal vent system.

Hydrothermal vents are extremely productive environments wherein primary production occurs via chemolithoautotrophy, the generation of energy for carbon fixation from the oxidation of vent-derived reduced inorganic chemicals (6). The dense communities of macrofauna that populate these habitats typically are dominated by invertebrates that form symbiotic associations with chemolithoautotrophic bacteria (7). In these chemosynthetic associations, the endosymbionts oxidize reduced vent-derived compounds—usually hydrogen sulfide (H_2S)—and fix inorganic carbon, which is shared with their host for biosynthesis and growth (8–12). Symbiotic associations between chemolithoautotrophic bacteria and invertebrates have been described for multiple invertebrate taxa from three phyla (13), and these associations often coexist within given vent fields, systems of vent fields (regions), and biogeographic provinces (14).

It is well established that hydrothermal fluid can exhibit marked spatial and temporal differences in temperature, pH, and chemical composition, the result of numerous subsurface geological, chemical, physical, and biological factors (15–18). This heterogeneity across both space and time provides myriad physicochemical niches and ample ecological opportunity to support a diversity of chemosynthetic symbioses via niche specialization. Previous studies have examined successional changes within a community of chemosynthetic symbioses in relation to temporal changes in vent-fluid chemistry (19, 20), the distribution of the symbioses in relation to physicochemical conditions within a vent field (21–27), and the distribution of chemosynthetic symbioses among different vent fields (28, 29). Host tolerance, growth rates, and physiological capacities often are invoked when explaining the observed distribution. Given the reliance of chemosynthetic symbioses on vent-derived chemicals for symbiont function (30), variations in symbiont physiological activity have the potential to result in distinct habitat-utilization patterns by holobionts. However, no study has yet comprehensively interrogated both

host and symbiont to ascertain whether there is evidence for symbiont-influenced niche partitioning at vents.

Despite a convergence of general function among chemosynthetic symbioses in which the endosymbionts provide primary nutrition for the host, chemolithoautotrophic symbiont lineages have evolved multiple times from distinct lineages of free-living Proteobacteria (13, 31), and the genetic distance within and among symbiont lineages is sufficient to posit that physiological differences exist among them. Indeed, ongoing studies of chemosynthetic symbioses continue to reveal diverse modes of energy metabolism, such as hydrogen and carbon monoxide oxidation (32, 33). Given the obligate nature of these associations, the ecological implications of differences in symbiont physiological capacity are quite significant, because they may enable niche partitioning that results in previously inexplicable or unrecognized distribution patterns. If there are physiological differences among the symbionts of given groups (genera or species) of hosts, symbiont physiological activity would have the potential to constrain host habitat utilization via differences in chemolithotrophic metabolism.

Provannid gastropods of the genus *Alviniconcha* provide a unique opportunity to study symbiont-driven host niche partitioning. *Alviniconcha* are widely distributed at vents in the western Pacific (Manus Basin, Marianas Trough, North Fiji Basin, and the Lau Basin) as well as in the Indian Ocean at vents along the Central Indian Ridge. In addition to the described species of *Alviniconcha*, previous studies have found additional host "types" which are sufficiently divergent that they may represent undescribed species (34–36). These species and host types have been observed to host either intracellular γ- or ε-proteobacterial symbionts in the gill (36–40). Studies of the distribution of these species and types among vent fields examined a modest number of specimens per site (e.g., two individuals from each sampling site), with little or no contextual habitat information. As such, it is impractical to infer from these data the relationship between host type, symbiont type, and habitat utilization.
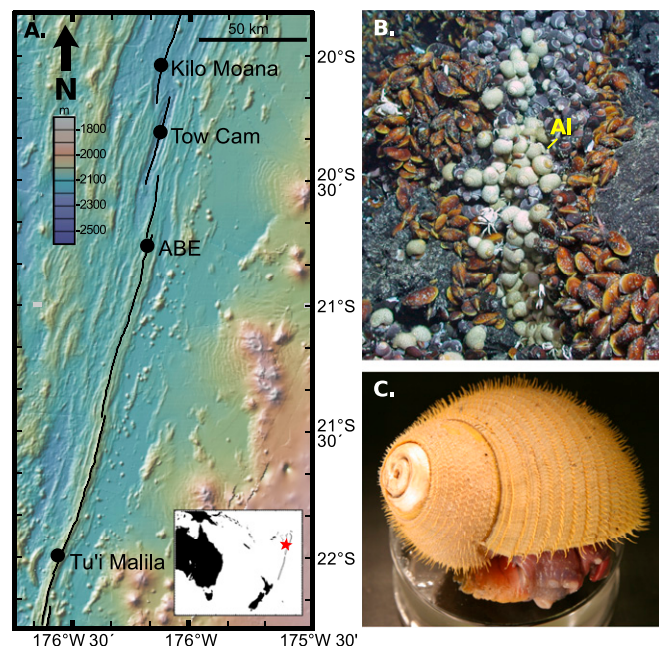
To look for patterns indicative of symbiont-influenced habitat partitioning, we collected 288 *Alviniconcha* individuals from the walls of hydrothermal chimneys and diffuse-flow habitats (where hydrothermal fluid is emitted from cracks in the seafloor) (Fig. 1 and Table S1). *Alviniconcha* were sampled from four vent fields spanning a regional geological gradient, where the two northernmost fields (Tow Cam and Kilo Moana) are dominated by basaltic lava, and the two southernmost vents (ABE and Tu'i Malila) are dominated by andesitic lava (41–45). Coregistered measurements of the physicochemical habitat within the animal collections, as well as characterization of vent end-member fluids from within each field, provide contextual geochemical information for these samples. Both host and symbionts were subject to phylogenetic analyses, and the composition of the symbiont population of all individuals was determined via quantitative PCR (qPCR). Select samples were also analyzed for stable-carbon isotopic content. Collectively, these data reveal striking patterns of both host and symbiont (holobiont) distribution along an ∼300-km length of the ELSC. The observed patterns in holobiont distribution correlate with differences in vent-fluid composition along the ELSC, implicating *Alviniconcha* symbionts in governing the distribution of their hosts among vent fields. These data provide evidence that symbiont complement might influence niche partitioning within a closely related group of animals and might in this case, as a consequence of differences in geochemical composition along the entire spreading center, yield regional-scale patterns of holobiont distribution.

Results

Phylogenetic Analysis of the Host Mitochondrial Cytochrome C Oxidase Subunit 1 Gene. We successfully amplified partial mitochondrial cytochrome C oxidase subunit 1 (CO1) from 274 host individuals and recovered a total of 56 haplotypes (Table S2). These haplotypes were distributed among three major clades with high (>0.95) posterior support, corresponding to three host types from the southwestern Pacific, and are called type 1 (HT-I), type 2 (HT-II), and type Lau (which we renamed here HT-III) (Fig. 2). Only HT-III has been previously described from the Lau Basin (38). Our results corroborate the *Alviniconcha* phylogeny as published in ref. 38, in which one major clade includes HT-I, HT-III, and *Alviniconcha hessleri* (from the Mariana trench), and the second major clade includes HT-II and *A. aff. hessleri* (from the Indian Ocean). For HT-I and HT-II, reference sequences AB235211 and AB235212 were each identical to the most common experimental haplotype in their respective clade; AB235215, representing HT-III, was identical to a relatively rare haplotype in our dataset but had only one nucleotide difference from the most common HT-III haplotype. The three host types found on the ELSC were divergent from those observed in the northwestern Pacific (Mariana Trench) and the Indian Ocean.

Some structure was apparent within the major host types in our sample. Within HT-III, a clade including 11 of the 22 HT-III haplotypes was supported with a posterior probability approaching 1.0. Although structure also was apparent in other host types, none was resolved with a posterior probability exceeding 0.9.

Phylogenetic Analyses of Symbiont 16S rRNA Genes. Based on 16S rRNA gene sequences, three symbiont phylotypes were found to be associated with ELSC *Alviniconcha*, only one of which had been previously observed in this region. Longer sequences were generated from clones of each phylotype for phylogenetic analysis (Fig. 3) and revealed that the three phylotypes are closely related to the previously published sequences for the γ- and ε-proteobacterial endosymbionts from *Alviniconcha* in this and other hydrothermal systems in the southwestern Pacific (Manus and North Fiji basins) (36–38). One of the γ-proteobacterial symbiont phylotypes, γ-Lau, was most closely related to the previously published symbiont sequence from *Alviniconcha* in the Lau Basin

Fig. 1. (*A*) Map of ELSC depicting the four vent fields sampled herein. (*Inset*) Location of ELSC in the South Pacific. (*B*) A typical assemblage of *Alviniconcha* (AI) and other vent animals in the Lau Basin (Image courtesy of James Childress, University of California, Santa Barbara). (*C*) An individual *Alviniconcha* snail.
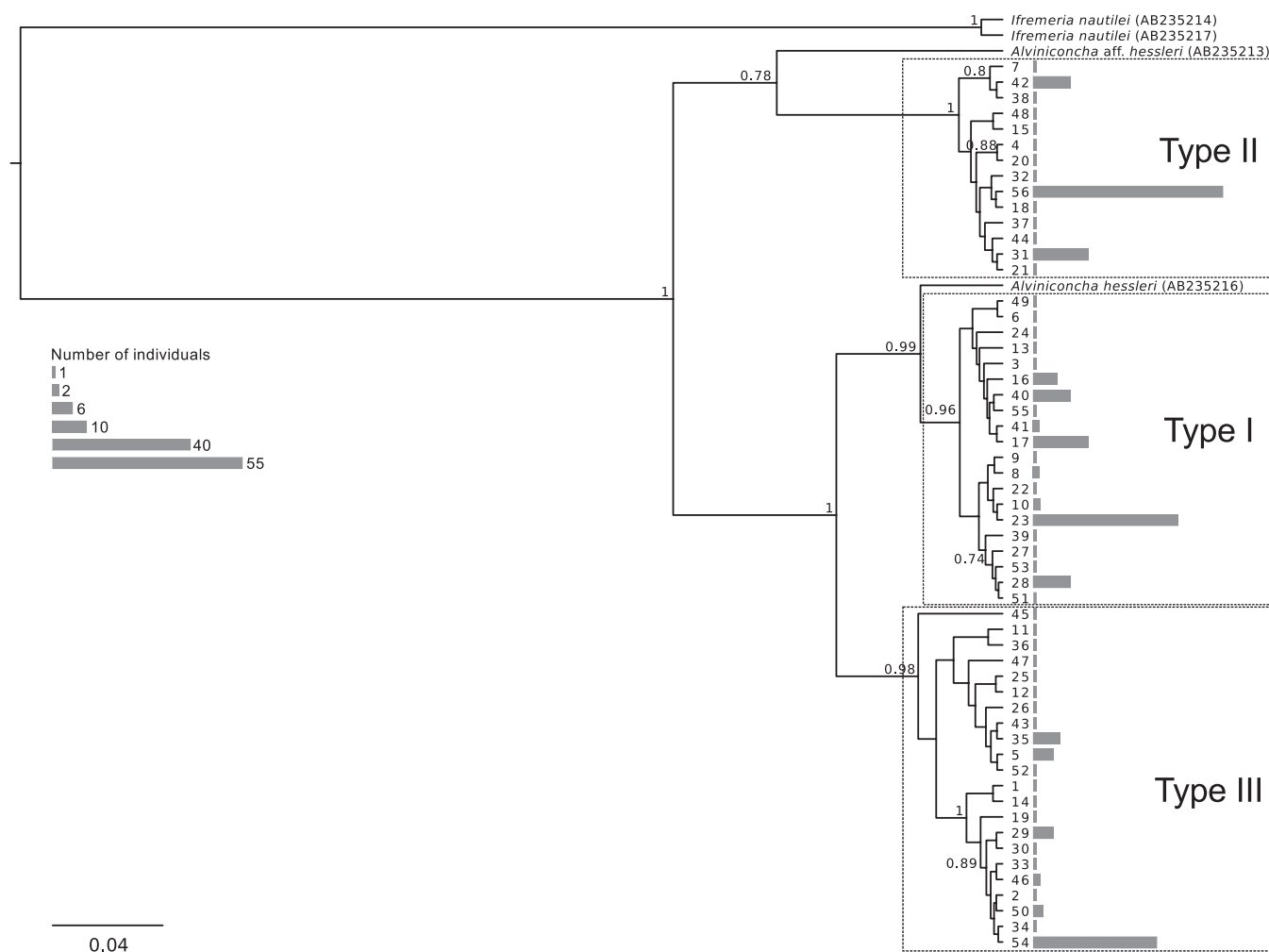
Fig. 2. Bayesian inference phylogeny of the *Alviniconcha* host mitochondrial CO1 haplotypes from this and previous studies and sequences from the sister genus *Ifremeria*. Boxes show the three *Alviniconcha* host types reported here. The haplotype ID number is shown at the tip of each branch, and the gray bars represent the total number of individuals recovered for each haplotype. Accession numbers for haplotypes found in this study are given in Table S2. Posterior probabilities are indicated above the nodes if >0.7.

(98% sequence identity) (38). The second γ-proteobacterial symbiont, phylotype γ-1, and an ε-proteobacterial symbiont phylotype were most closely related (96–97% and 97% sequence identity, respectively) to *Alviniconcha* symbionts previously observed in the North Fiji and Manus basins (38).

Proportion of Symbiont Phylotypes Within *Alviniconcha*. Quantification via qPCR revealed that all *Alviniconcha* individuals analyzed were dominated (>67% of total detected 16S rRNA genes) by either γ- or ε-proteobacterial endosymbionts. The dominant phylotype on average represented 99.5 ± 2.2% of the total symbiont gene counts within all individuals (Fig. 4). We never observed individual snails with approximately equal representation of γ- and ε-proteobacteria, although we did observe individuals with roughly equal representation of the two γ-proteobacterial phylotypes. Accordingly, we refer to *Alviniconcha* individuals as primarily hosting either γ- or ε-proteobacterial endosymbionts.

Relationships Among Symbiont Phylotypes and Host Types. Our qPCR analysis also revealed specificity among the three host types and three symbiont phylotypes. One-way analysis of similarity (ANOSIM) comparing the symbiont composition among the different host types demonstrated that each host type associated with significantly different symbiont populations (global

$R = 0.789, P < 0.001$) (Fig. 4). HT-II were exclusively dominated by ε-proteobacteria, with ε-proteobacteria always representing >99% of the detected symbiont genes. Accordingly, we found no significant differences in the symbiont population among HT-II from three different vent fields (one-way ANOSIM; global $R = 0.312, P = 0.07$). HT-III, conversely, were exclusively dominated by γ-proteobacteria, either γ-1 or γ-Lau. A small number of HT-III individuals ($n = 7$, hereafter called "γ-Both") had relatively equal proportions of both γ-proteobacterial phylotypes. HT-III was found at the two southernmost vent fields (ABE and Tu'i Malila); however, because of the presence of only one HT-III individual at ABE, we were unable to statistically test the effect of geography on symbiont population composition in this host type. Finally, HT-I was dominated by either γ-1 or ε-proteobacteria but moret commonly dominated by γ-1, not the ε-proteobacteria ($n = 93$ vs. 6 individuals respectively). In this host type, the associated symbiont population displayed different patterns of symbiont fidelity according to geography. HT-I was found at all four vent fields; however, the dominant symbiont phylotype changed from north to south. Five of 12 HT-I individuals in the northern vent fields were dominated by ε-proteobacteria, compared with only 1 of 87 HT-I individuals in the southern vent fields. This finding was confirmed via one-way ANOSIM comparing the symbiont population of HT-I by location, which
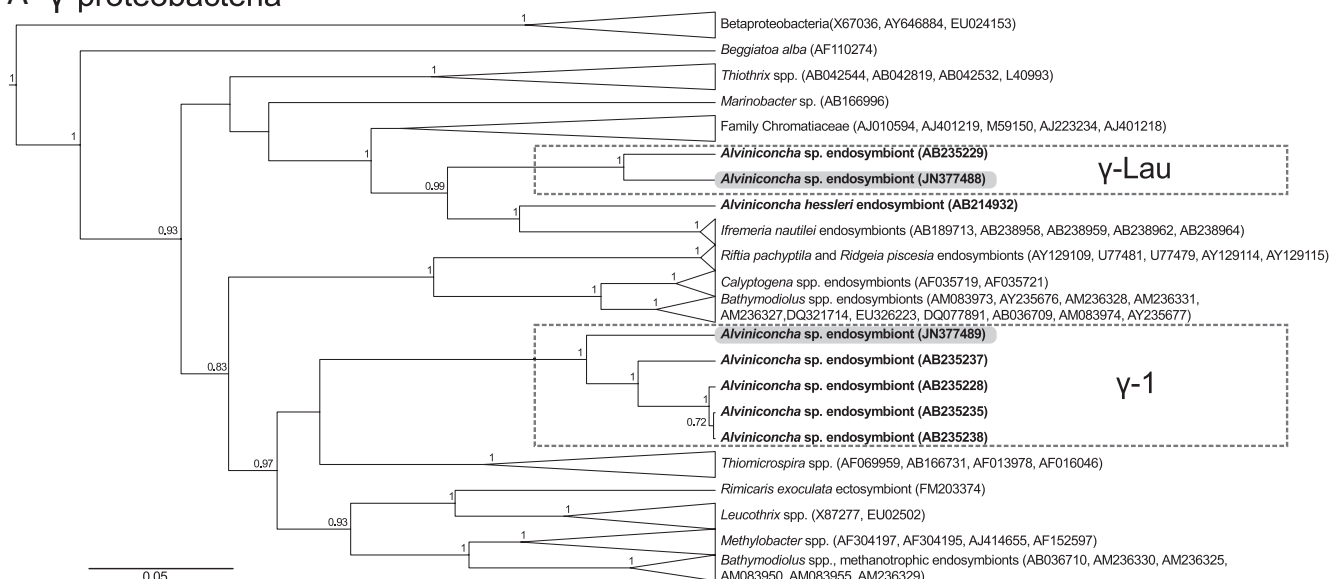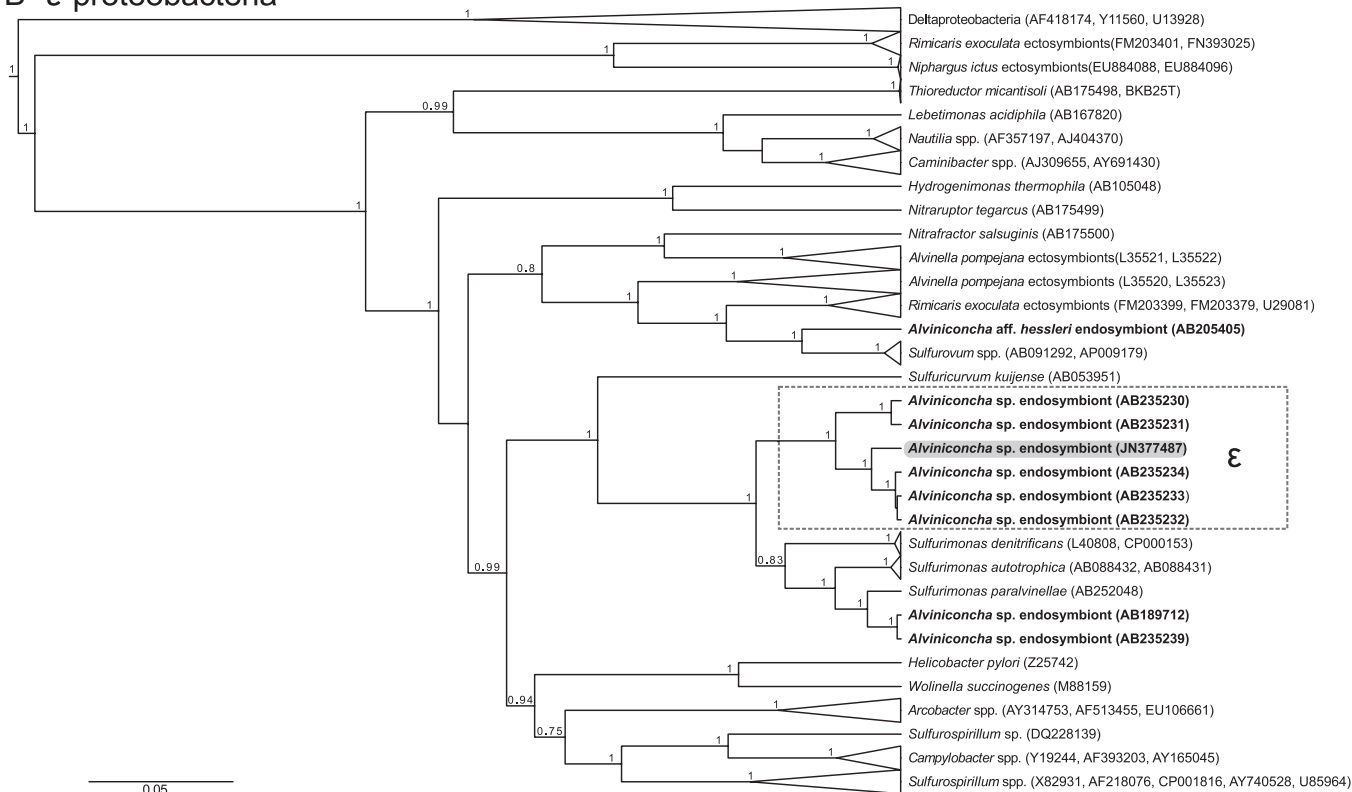
Fig. 3. Bayesian inference phylogenies of 16S rRNA sequences showing the three *Alviniconcha* symbiont phylotypes found at the ELSC. All *Alviniconcha* symbionts, from this study and others, are shown in bold. Gray highlighting indicates the representative sequences from this study. Boxes show the *Alviniconcha* symbiont phylotypes defined here and in other studies. Posterior probabilities are indicated above the nodes if >0.7. (*A*) γ-proteobacterial phylogeny, with β-proteobacteria as the outgroup. (*B*) ε-proteobacterial phylogeny, with δ-proteobacteria as the outgroup.

demonstrated that there were significant differences among HT-I individuals from the different vent fields (global $R = 0.385$, $P < 0.001$).

Geographic Patterns in the Abundance of *Alviniconcha* Host Types. The distribution and abundance of each host type varied geographically from north to south (Fig. 5). HT-I was found at all

four vent fields, HT-II was found at three vent fields but not Tu'i Malila, and HT-III was found at the two southernmost vent fields, ABE and Tu'i Malila. With respect to their relative abundance, *Alviniconcha* populations at the northern vent fields were mainly HT-II, whereas populations at the southern vent fields were mainly HT-I and HT-III. The relative abundances of host types in the two northern vent fields (Kilo Moana and Tow
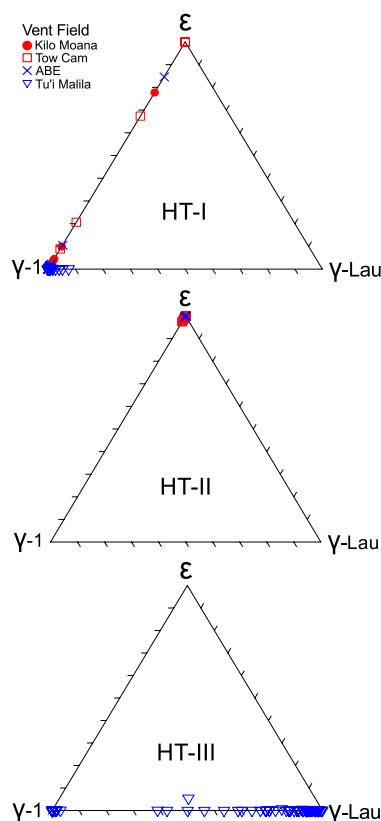
Fig. 4. Ternary plots of the symbiont composition of each *Alviniconcha* host type, with each point showing the symbiont composition of a single individual. The vertices of the triangle represent 100% of each symbiont phylotype, and the tick marks on the axes represent decreasing intervals of 10%. The symbiont phylotypes are indicated by γ-1 (γ-proteobacteria type 1), γ-Lau (γ-proteobacteria type Lau), and ε (ε-proteobacteria). Vent fields are indicated by ● (Kilo Moana), □ (Tow Cam), X (ABE), and ▽ (Tu'i Malila).

Cam) versus two southern vent fields (ABE and Tu'i Malila) were significantly different (global $R = 0.34$, $P = 0.03$).

Geographic Abundance of Symbiont Phylotypes. The abundance of symbiont phylotypes associated with *Alviniconcha* changed along the spreading center (Fig. 5). Individuals dominated by symbiont γ-1 were present at all four vent fields. Individuals dominated by ε-proteobacteria were present three vent fields but not Tu'i Malila. Individuals dominated by γ-Lau were observed only at Tu'i Malila. The dominant symbiont phylotypes in *Alviniconcha* from the two northern vent fields (Kilo Moana and Tow Cam) were significantly different from those of the southern two vent fields (ABE and Tu'i Malila) (one-way ANOSIM, global $R = 0.409$, $P = 0.024$). Specifically, the majority of *Alviniconcha* at the northern vent fields (Kilo Moana and Tow Cam) were dominated by ε-proteobacteria, whereas the majority of *Alviniconcha* at the southern vent fields (ABE and Tu'i Malila) were dominated by one of the two γ-proteobacterial phylotypes.

Chemistry and Temperature at *Alviniconcha* Habitats. Chemical and thermal measurements were taken upon the cleared substratum after *Alviniconcha* collections were completed (Table S1 and Fig. 6). Free sulfide concentrations in the vent fluids of the northernmost *Alviniconcha* habitats were significantly greater than those of the southernmost habitats (Mann–Whitney U, $P = 0.038$). Although we happened to sample more chimney wall habitats in the north, this difference in sampling does not explain the significant difference in sulfide concentrations between

northern and southern fields. Indeed, when grouped by habitat type regardless of region, diffuse flows and chimney wall habitats measured here did not have significantly different sulfide concentrations (Mann–Whitney U, $P = 0.126$) (Table S1 and Fig. 6), nor did diffuse flows and chimneys within the same region (Mann–Whitney U, $P = 0.182$ and $P = 0.102$, north and south respectively). We also did not detect any significant differences in the oxygen concentrations or temperature of the vent fluids among the sample collection sites in the northern and southern vent fields ($P = 0.180$ and $P = 0.118$ respectively).

End-Member Vent-Fluid Chemistry. End-member aqueous concentrations of H_2S and hydrogen (H_2) reveal along-axis geochemical variations from north to south (Fig. 7). End-member aqueous H_2 concentrations varied from 220–498 µM in the northernmost vents (at Kilo Moana) and decreased to concentrations that varied from 35–135 µM in the southernmost (at Tu'i Malila) vents, nearly an order-of-magnitude difference in concentration. End-member dissolved H_2S concentrations exhibit a similar trend from north to south, although the ~twofold change in concentration of 4.9–2.8 mM from north to south is substantially
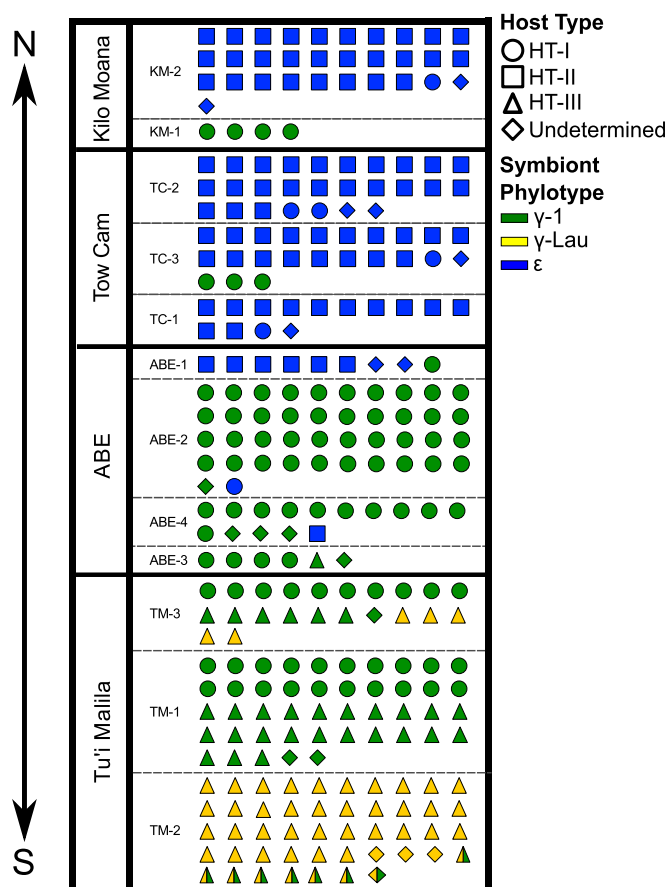
Fig. 5. The distribution of *Alviniconcha* host types and dominant symbiont type across the ELSC, with each individual colored according to dominant symbiont phylotype (>67% of the total detected 16S rRNA genes) and shaped according to host type. The four vent fields are separated by solid lines, and distinct collections from within each vent field are divided by dashed lines, with the collection ID indicated (Table S1). Symbiont phylotypes are indicated as follows: green, γ-proteobacteria type 1 (γ-1); yellow, γ-proteobacteria type Lau (γ-Lau); blue, ε-proteobacteria (ε).The individuals that had relatively equal proportions of two of the symbiont phylotypes are shown as two colors. Host types are indicated by shapes: ●, host type 1 (HT-I); ■, host type II (HT-II); ▲, host type III (HT-III); ◆, host type undetermined.

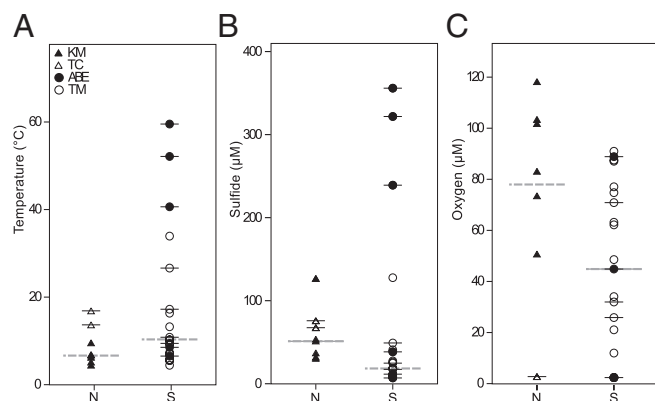**Fig. 6.** Cyclic voltammetry measurements made on the cleared substratum after *Alviniconcha* collections, showing (*A*) temperature, (*B*) free sulfide concentration (sulfide), and (*C*) oxygen concentration at northern collections versus the southern collections. North (N) includes the vent fields Kilo Moana (KM) and Tow Cam (TC); South (S) includes ABE and Tu'i Malila (TM). Symbols with horizontal lines represent samples from diffuse vent flows; symbols without lines represent chimney wall habitats. Median values for each region are indicated by a dashed horizontal line.

less than that observed for aqueous H_2. In contrast to H_2 and H_2S, end-member methane (CH_4) concentrations in 2009 occupied a very narrow range of 33–44 μM and showed no along-axis trends (Fig. 7). End-member aqueous dissolved inorganic carbon (DIC) concentrations were highest in the Tu'i Malila vent fluid, reaching a value of 15 mM, and lowest in ABE vent fluids where concentrations varied from 5.4–7.0 mM, with fluids from the other vent fields containing intermediate concentrations of DIC (Fig. 7). End-member CH_4 and DIC concentrations did not change markedly from 2005 to 2009.

Stable Carbon Isotopic Composition According to Dominant Symbiont Phylotype. Across the ELSC, the average $\delta^{13}C$ value for gill tissue from *Alviniconcha* dominated by ε-proteobacteria ($-11.6 \pm 0.4‰$) was much less depleted than the average value of *Alviniconcha* dominated by γ-proteobacteria ($-27.6 \pm 2.3‰$) (Table S3). A one-way ANOVA of Tu'i Malila γ-proteobacteria hosting

Fig. 7. The end-member fluid concentrations of (*A*) H_2, (*B*) H_2S, (*C*) CH_4, and (*D*) DIC at the four vent fields along the ELSC from which *Alviniconcha* were collected. Symbols indicate year of sampling: X, 2005; ●, 2009. DIC and H_2S data from 2005 were published previously by Mottl et al. (44).

individuals grouped by dominant symbiont phylotype (γ-1, *n* = 23; γ-Lau, *n* = 21; γ-Both, *n* = 8), irrespective of host type, showed that there were significant differences among the groups ($P < 0.001$). Tukey's multiple pairwise comparisons showed that the $\delta^{13}C$ value in individuals dominated by γ-Lau was not significantly different from that in γ-Both individuals ($P = 0.834$), whereas individuals dominated by either γ-Lau or γ-Both were significantly less depleted than individuals dominated by γ-1 ($P = 0.001$ and $P = 0.004$, respectively). We were unable to compare the possible effects of host type on the stable-carbon isotopic composition in this subset of individuals, because we did not have enough individuals of different host types with the same dominant symbiont phylotype for statistical analysis.

Discussion

These analyses, which were based on an extensive sampling effort in four different vent fields along the length of the ELSC, uncover previously cryptic, regional-scale patterns in the distribution of *Alviniconcha* holobionts. Our results suggest that regional-scale gradients in geochemistry, which are the surficial expression of subsurface tectonic processes and water–rock interactions, respectively, influence niche availability—and thus partitioning—among hydrothermal vent symbioses. Specifically, we observed striking patterns in the distribution of *Alviniconcha* host types, wherein *Alviniconcha* associated with ε-proteobacteria were substantially more abundant at the northernmost, basaltic vent fields (Kilo Moana and Tow Cam). Conversely, *Alviniconcha* associated with γ-proteobacteria were more abundant at the andesitic southern vent fields (ABE and Tu'i Malila) (42, 43). We observed further basin-wide geographic trends in *Alviniconcha* individuals hosting different γ-proteobacterial symbionts, including the absence of individuals dominated by the γ-Lau phylotype from all except the Tu'i Malila vent fields. Together, with geochemical data from high-temperature and diffuse vent fluids from these vent fields, our results indicate that niche partitioning within a genus of chemosynthetic symbioses at deep sea hydrothermal vents is linked to subsurface geological/geochemical processes. These data suggest that interactions between symbionts and the physicochemical habitat, rather than host physiology alone, can govern the distribution of hydrothermal vent symbioses across a biogeographical province.

Symbiont and Host Diversity and Association. The cryptic diversity revealed here reshapes our understanding of the biogeography of this genus. Before this study, only HT-III (previously called "host type Lau") and one symbiont phylotype (γ-Lau) had been documented in the Lau Basin (38). Our phylogenetic surveys uncovered two additional host types (HT-I and HT-II) and two additional symbiont phylotypes (γ-1 and ε-proteobacterial) within the ELSC. Collectively, these data establish the ELSC as the geographic area with the highest documented diversity for this genus, with a greater number of host types and symbiont phylotypes than in any other region. [It is possible that *Alviniconcha* hosts and symbionts are comparably diverse at other western Pacific and Indian Ocean vent systems, although this remains to be determined (36–38, 40).] Regardless, the data herein show unforeseen holobiont diversity within the genus *Alviniconcha* and emphasize the value of interrogating both host and symbiont identity at an appropriate sampling scale to capture cryptic phylogenetic diversity.

The observed patterns of association among the host and symbiont phylotypes were most surprising. 16S rRNA gene qPCR of all sampled individuals revealed that *Alviniconcha* host types exhibited varying degrees of specificity for their symbionts. *Alviniconcha* HT-II associated solely with ε-proteobacteria. HT-III hosted mixed populations of the two γ-proteobacterial phylotypes (γ-Lau and γ-1). Notably, HT-I associated with both γ- or ε-proteobacterial endosymbionts, sometimes within the same individual (although one endosymbiont always dominated).
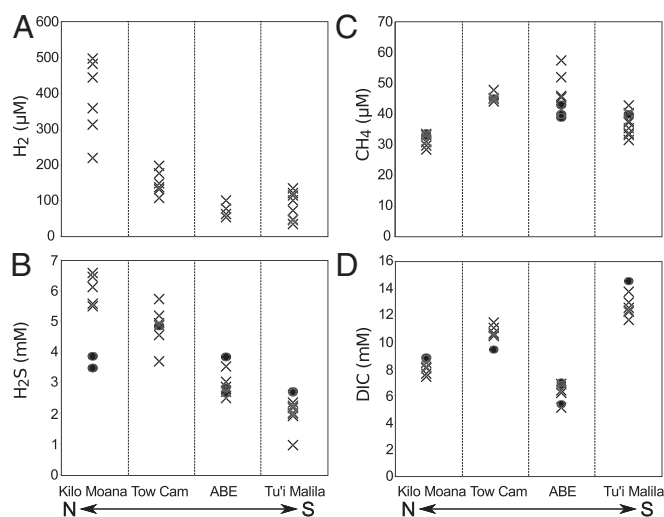
Although some species of *Bathymodiolus* hydrothermal vent mussels are known to associate with two endosymbiotic γ-proteobacterial phylotypes (46–48), the ability of an *Alviniconcha* individual to host endosymbionts from two distinct bacterial classes is unprecedented among chemosynthetic symbioses. These symbionts are thought to be environmentally acquired (49), and the observed patterns of symbiont distribution among host types suggest interplay between host specificity and environmental determinants. This interplay may have a profound role in structuring the distribution of *Alviniconcha* host types across available niche space.

Holobiont Distribution and Basin-Wide Geochemical Gradients. Further investigation revealed that the holobionts exhibited a structured pattern of distribution across the four vent fields. Although *Alviniconcha* HT-I and the symbiont γ-1 were represented at all four vent fields, individuals dominated by the symbiont γ-Lau were observed at only one vent field (Tu'i Malila), and only one HT-III individual was found outside of Tu'i Malila. Structured distributions of marine fauna often result from geographical isolation or other barriers to dispersal (50, 51). However, the representation of host HT-I and symbiont phylotype γ-1 among all of the vents studied here, combined with our recovery of host haplotypes identical to previously collected individuals from thousands of kilometers away, suggests that the existence of such barriers is unlikely. *Alviniconcha* are thought to produce far-dispersing planktotrophic larvae (52), and studies of deepwater circulation in the ELSC have revealed continuity among the sites (53). Thus, the potential for geographic isolation caused by limitations on larval dispersal or deepwater circulation along the ELSC seems low.

Geological and geochemical gradients along the spreading center better explain the observed holobiont distributions. The ELSC comprises a series of vent fields in the Lau back-arc basin created by the subduction of the Pacific plate under the Indo-Australian plate. As the ELSC proceeds from north to south, it approaches the volcanic arc, resulting in an increased influence of the subducting Pacific plate on the crustal rocks (54–56). Consequently, there is a change in crustal rock type, with vent fields in the north being dominated by basalt and vent fields in the south being dominated by basaltic-andesite and andesitic lavas (42, 43). The increasing influence of the subducting slab is reflected in the changing geochemical composition of vent fluids north to south along the spreading center, including sizeable differences in dissolved volatile concentrations (28, 44, 45). Our analyses of high-temperature vent effluents from among the sampling sites revealed variations in gross geochemical composition along the ELSC that appear to be stable over time (44, 45). Both H_2 and H_2S concentrations decrease from north to south, with H_2 showing about an order-of-magnitude difference in concentration in end-member fluids from Kilo Moana in the north (~500 μM) to Tu'i Malila in the south (~43 μM). Because there often is a correspondence between the geochemical composition of a diffuse flow and nearby high-temperature flow (57–59), the elevated H_2 and H_2S concentrations in the high-temperature fluids at the northern vent sites likely correspond to higher concentrations of these chemical species in the cooler vent fluids bathing the *Alviniconcha* at these fields. Indeed, in situ voltammetry of vent fluids from among the collections corroborated the above geochemical trend and established that sulfide concentrations were higher among the *Alviniconcha* aggregations in the northern vent fields, although temperature and oxygen concentrations were not significantly different among the collection sites.

Niche Partitioning. If there are functional differences among *Alviniconcha* symbionts, then each host type's specificity for a particular symbiont would influence its capacity to exploit different physicochemical niches. Given the aforementioned distribution of phylo-

types and the seeming lack of barriers to dispersal, we posit that the observed patterns of distribution of *Alviniconcha* across the ELSC relates to the gradients in vent-fluid geochemistry (Fig. 7). Holobionts with ε-proteobacterial symbionts dominated in fields with higher H_2 and H_2S concentrations, and conversely holobionts with γ-proteobacterial symbionts were in greater abundance at fields with lower H_2 and H_2S. This observation is consistent with studies of free-living ε- and γ-proteobacteria in sulfidic environments, which found that ε-proteobacteria dominate over γ-proteobacteria in habitats with higher sulfide (60–62). Both H_2 and sulfur oxidation are known to be common metabolisms among the close relatives (i.e., *Sulfurimonas* spp.) of the ε-proteobacterial symbionts (60, 63–65), and we hypothesize that one or both of these mechanisms supports autotrophy in this phylotype. Previous studies of *Alviniconcha* symbiont metabolism have focused on sulfide oxidation in vivo and in vitro (39, 66) but did not identify the symbionts, so it is unclear which phylotypes are engaged in this metabolism. We observed that holobionts with ε-proteobacteria did not have visible sulfur granules (a known intermediate in some sulfur oxidation pathways) in their gills. In contrast, holobionts with γ-proteobacteria had elemental sulfur in their gills, suggesting different modes of sulfur metabolism. This finding, too, is consistent with studies of sulfur oxidation by ε- and γ-proteobacteria, which are known to use different pathways (reviewed in ref. 60). We recognize that other factors, yet to be determined, could influence the north-to-south partitioning of ε- and γ-proteobacterial symbionts as well as the distribution of holobionts with γ-Lau and γ-1, along the ELSC. Further work identifying the specific reductants and pathways used by the three symbiont phylotypes is needed to better understand the connection between symbiont physiology and the observed habitat partitioning.

We also observed evidence for niche partitioning at a local (vent-field) scale. Most collections were dominated by holobionts associating with one particular symbiont type (e.g., HT-I and II both hosting ε-proteobacterial symbionts in collection TC-2) (Fig. 5). This patchiness does not correspond strictly to habitat type (chimney wall vs. diffuse flows), because collections from both habitat types were dominated by ε-proteobacterial symbionts in the north and, conversely, by γ-proteobacterial symbionts in the south. There are anomalous collections from Kilo Moana and ABE that deviate from the overarching patterns of distribution in this study and that reflect local patchiness in geochemistry. Indeed, if these patterns are driven by habitat conditions, we would expect local variation in chemistry to result in patchy holobiont distribution even within a vent field. Unfortunately, we did not collect environmental data at these specific sites, so we cannot determine whether these collections were associated with different geochemistry. Although higher-resolution sampling of *Alviniconcha* with associated fine-scale chemical measurements is necessary to understand the extent of intrafield habitat partitioning by these symbioses, the existing data suggest interactions between the symbionts and the environment.

Previous studies have hypothesized that differences in the oxygen tolerance of the carbon fixation pathways used by the γ- and ε-proteobacterial symbionts could influence habitat utilization by the different *Alviniconcha* symbioses (38, 61). Indeed, our measurements of carbon-stable isotopic composition are consistent with the use of different carbon-fixation pathways by the γ- and ε-proteobacterial symbionts (Table S3). However, the oxygen concentrations were not significantly different in the habitats occupied by individuals with the γ- and ε-proteobacterial symbionts. Moreover, it is unlikely that environmental oxygen concentrations are experienced by the symbionts, because host oxygen-binding proteins, such as the gill hemoglobin of *Alviniconcha* (67), have a high affinity for oxygen and will govern its partial pressure within the host's tissues. With respect to whether differences in host physiology influence the observed distribution patterns, little is known about differences in thermal tolerance or

chemotolerance among *Alviniconcha* host types (66). Sulfide tolerance has been suggested to affect animal distribution at vents (23, 27, 68) and is significantly different among collections dominated by the different *Alviniconcha* holobionts at the ELSC. However, the highest sulfide levels detected among the snails in our collections are well below the tolerance limits reported from shipboard experiments on *Alviniconcha*, and thus host tolerance for sulfide is unlikely to be responsible for the patterns we report (66). Additionally, temperature and oxygen concentrations—two key factors often invoked in governing the distribution of animals at vents (23)—were not significantly different among our collection sites. Although both host and symbiont physiology undoubtedly influence the overall niche of these holobionts, we suggest that host physiology is unlikely to play a major role in the habitat partitioning observed here.

Conclusions

For vent holobionts, access to vent-derived chemical resources (reduced compounds for chemolithoautotrophy) requires physical proximity to the emitted vent fluid, as evidenced by the strong association of chemosynthetic symbioses with vent-fluid emissions (e.g., ref. 28). Competition among these holobionts for chemical resources takes the form of competition for the limited space near vent flows. Within a chemically heterogeneous vent system such as the ELSC, with spatial variability in the composition of vent fluid, resource partitioning among symbioses appears to occur via the differential distribution of the symbioses across the range of geochemical milieus. Here, we observed this process occurring both within a genus and at a regional scale, with differential distribution of holobionts among distinct vent fields that are tens of kilometers apart.

In many ecosystems, niche partitioning has been shown to facilitate the coexistence of ecologically similar taxa (reviewed in ref. 3) but generally has been considered in the context of the intrinsic differences in organisms, not in differences in their symbionts. Despite growing knowledge of the ubiquity of symbioses in the natural world, evidence for their effects on niche partitioning among similar hosts is surprisingly rare. In a few animal–microbial symbioses, namely coral–algal and aphid–bacterial associations, studies have correlated microbial symbiont genetic and physiological diversity with niche partitioning by the symbioses. In these cases, specificity in partnering among physiologically distinct endosymbiont phylotypes and genetically distinct hosts has been found to correspond to the distribution of corals in different light and temperature regimes on reefs (69–74) and to the distribution of aphids on different plant types (75–77). Previous research on the relationship between symbiont identity and environmental geochemistry at hydrothermal vents examined how differences in symbiont phylotype and abundance varied within a single species of mussel as a function of habitat (47, 78–80). It now is apparent that the process of symbiont-influenced niche partitioning among genetically distinct hosts is likely to play a role in structuring vent ecosystems and is driven by subsurface geological and geochemical interactions. The influence of symbiont metabolism on host niche utilization is fundamental to our understanding of hydrothermal vent symbioses and vent ecosystems. With increasing awareness of the prevalence of microbe–animal interactions in our biosphere, the process of symbiont-driven niche partitioning is likely to be elemental in other biological systems as well.

Methods

Alviniconcha Specimens. A total of 288 *Alviniconcha* specimens were collected from four vent fields in the ELSC using the remotely operated vehicle (ROV) *Jason II* during expedition TM-235 in 2009 on board the R/V *Thomas G. Thompson* (Fig. 1 and Table S1). Sites were chosen randomly, and live specimens were collected using modified "mussel pots" (81, 82) or large scoop nets and were returned to the ship in insulated containers. On board ship, live specimens were kept in chilled (4 °C) seawater until dissection. Symbiont-

containing gill tissues were dissected on shipboard and were frozen immediately at –80 °C. The frozen tissue remained at –80 °C until it was subsampled for DNA extraction and carbon isotope analysis.

Free Sulfide, Oxygen, and Temperature Determination via in Situ Voltammetry. In situ voltammetry and a temperature probe were used to determine free sulfide and oxygen concentrations as well as fluid temperatures associated with a subset of the *Alviniconcha* collections (Table S1) (83, 84). Measurements were made in the same manner for both diffuse flows and chimney walls. Briefly, animals were collected, and then 1–12 scan sets were performed with the tip of the probe directly on the cleared substrate. Each scan set was comprised of 7–12 discrete measurements (scans), which then were averaged. At the diffuse-flow sites, measurements were made on the cleared substratum after animals were collected. At the chimney wall sites, after animals were collected, the probe was positioned directly along the side of the perpendicular to chimney wall structure, so that the tip touched or was within 1 cm of touching the chimney wall (based on the laser scale from the ROV *Jason*). In all cases, shimmering water often was visible, and temperatures never were higher than 60 °C. The instrument's quantitative limits of detection for free sulfide and oxygen are 0.2 μM and 15 μM, respectively. For statistical analyses, values below the quantitative limits of detection were treated as in ref. 28.

End-Member Vent-Fluid Sampling and Analyses. Hydrothermal fluids were recovered from high-temperature orifices (temperatures ranged from 268–320 °C) using the ROV *Jason II* and isobaric gas-tight fluid samplers (85) during expedition TM-236 in June–July 2009 on the R/V *Thomas G. Thompson*. Samples were analyzed for dissolved CH_4, H_2S, and DIC. Dissolved CH_4, DIC, and H_2 also were measured at the vent fields sampled during this study during expedition TUIM05MV on the R/V *Melville* (April–May 2005) (see ref. 44 for 2005 sample information). All fluid samples were processed via gas chromatography or gravimetry as in ref. 44. See *SI Methods* for details of end-member calculations.

DNA Extraction. Approximately 25 mg of gill tissue was subsampled while frozen for DNA extraction. Each subsample was placed into one well of a 96-well plate containing a proprietary lysis buffer from the AutoGenprep 965/960 Tissue DNA Extraction kit (AutoGen, Inc.), and DNA was extracted with the AutoGenprep 965 automatic extraction system. Before downstream analysis, all DNA extracts were diluted 1:100 in molecular-grade sterile water to minimize the effect of any coextracted inhibitors on downstream molecular analysis.

Phylogenetic Analysis of the Host Mitochondrial CO1 Gene. DNA extracts from all *Alviniconcha* individuals were used as template to partially amplify the CO1 mitochondrial gene, and the resulting sequences were cleaned, trimmed, and aligned and then were used to produce a Bayesian inference phylogeny using the SRD06 model of nucleotide evolution (86), which partitions the protein coding sequence into first plus second and third codon positions, estimating parameters for each. Details of these analyses can be found in *SI Methods*. Host CO1 gene sequences were deposited in GenBank, and accession numbers are given in Table S2.

Phylogenetic Analysis of Symbiont 16S rRNA Genes. Universal bacterial primers were used to amplify symbiont 16S rRNA genes from the DNA extracts of 30 individuals from ABE and Tu'i Malila. A clone library was constructed from the pooled amplicons of individuals from each vent field, and sequence diversity was assessed via partial sequencing of clones (see *SI Methods* for GenBank accession numbers). The clones were found to represent three phylotypes with >96% identity to previously sequenced *Alviniconcha* symbionts. Bidirectional sequencing of clones representative for each symbiont phylotype yielded longer sequences (accession numbers JN377487, JN377488, JN377489), which were cleaned, trimmed, and aligned with other 16S rRNA gene sequences from both free-living and symbiotic Proteobacteria and then were used to produce a Bayesian inference phylogeny with BEAST (87) implementing the GTR+I+G model of substitution. Details of these analyses can be found in *SI Methods*.

Symbiont qPCR Assay Development. SYBR Green qPCR primers (Table S4) were designed for the three symbiont phylotypes using the aforementioned 16S rRNA gene alignment. Each phylotype assay was designed to target *Alviniconcha* symbiont 16S rRNA gene sequences from this study and others to capture intraphylotype sequence diversity. Details of qPCR assay design and optimization are given in *SI Methods*.

Assessing Symbiont Composition via qPCR. To confirm that our subsamples yielded symbiont populations typical of the entire gill, we took three subsamples (from either end and the middle of each gill) from the whole gills of six individuals, extracted DNA as described above, and found that the proportion of symbiont phylotypes varied by <1% among subsamples (Table S5). We accordingly estimated the proportion of each symbiont phylotype in the original *Alviniconcha* gill DNA extracts by applying all three qPCR assays to 2 μL of each sample (in duplicate), which were compared against duplicate standard curves and no-template controls and then were averaged to determine copy number. Reactions in which the cycle threshold (C_t) was greater than the C_t for the lowest standard (10 copies) were documented as zero copies. Additionally, all quantities were adjusted for amplification inhibition (*SI Methods*). Symbiont populations within an individual were assessed by assuming each 16S rRNA gene to represent a single symbiont genome (see *SI Methods* for discussion of this assumption).

Analysis of Carbon Isotopic Composition. Approximately 300 mg gill tissue was subsampled while frozen for carbon isotopic analysis. Samples were lyophilized for 24 h and then were acidified with 0.1 N HCl to remove any inorganic carbon contamination. The samples subsequently were dried for 24–48 h at 50–60 °C, homogenized to a fine powder, and sealed within tin capsules. The carbon isotopic composition was determined by combustion in an elemental analyzer (Eurovector, Inc.) and separating the evolved CO_2 by gas chromatography before introduction to a Micromass Isoprime isotope ratio mass spectrometer for determination of $^{13}C/^{12}C$ ratios. Measurements are reported in δ-notation relative to the Peedee belemnite in parts per thousand deviations (‰). Typical precision of analyses was ±0.2‰ for $δ^{13}C$. Egg albumin was used as a daily reference standard.

Statistical Analyses. Comparisons of the symbiont composition of *Alviniconcha* individuals at different vent fields and among the four host types was assessed via ANOSIM using Bray–Curtis dissimilarity (88) (see *SI Methods* for details of ANOSIM). In these analyses, the symbiont composition for each individual represented an independent community profile. Additionally, the collections were compared by classifying each individual based on its dominant symbiont phylotype (γ-1, γ-Lau, ε, or γ-Both for the few individuals that hosted relatively equal proportions of the two γ-proteobacterial symbionts). In these analyses, Bray–Curtis dissimilarity from standardized collection profiles was used.

One-way ANOVAs with post hoc pairwise comparisons (Tukey's) were performed (SPSS Statistics v19) to compare the average carbon-stable isotope values among individuals from the same vent field (Tu'i Malila) with different dominant γ-proteobacterial symbiont phylotypes.

To compare the temperature and environmental sulfide and oxygen concentrations among the collections at all sites as measured via cyclic voltammetry, a nonparametric test (Mann–Whitney U; SPSS Statistics v19) was used.

1. Chase JM, Leibold MA (2003) *Ecological Niches: Linking Classical and Contemporary Approaches* (Univ of Chicago Press, Chicago).
2. Leibold MA, McPeek MA (2006) Coexistence of the niche and neutral perspectives in community ecology. *Ecology* 87(6):1399–1410.
3. Chesson P (2000) Mechanisms of maintenance of species diversity. *Annual Review of Ecology and Systematics* 31:343–366.
4. Schoener TW (1974) Resource partitioning in ecological communities. *Science* 185 (4145):27–39.
5. Schoener TW (1986) Resource partitioning. *Community Ecology: Pattern and Process*, eds Kikkawa J, Anderson DJ (Blackwell Scientific Publications, Boston), pp 91–126.
6. Fisher CR, Takai K, Le Bris N (2007) Hydrothermal vent ecosystems. *Oceanography (Washington DC)* 20(1):14–23.
7. Van Dover CL (2000) *The Ecology of Deep-Sea Hydrothermal Vents* (Princeton Univ Press, Princeton).
8. Cavanaugh CM, Gardiner SL, Jones ML, Jannasch HW, Waterbury JB (1981) Prokaryotic cells in the hydrothermal vent tube worm *Riftia pachyptila* Jones: Possible Chemoautotrophic Symbionts. *Science* 213(4505):340–342.
9. Fisher CR, Childress JJ, Minnich E (1989) Autotrophic carbon fixation by the chemoautotrophic symbionts of *Riftia pachyptila*. *The Biological Bulletin* 177(3):372–385.
10. Felbeck H (1981) Chemoautotrophic potential of the hydrothermal vent tube worm, *Riftia pachyptila* Jones (Vestimentifera). *Science* 213(4505):336–338.
11. Belkin S, Nelson DC, Jannasch HW (1986) Symbiotic assimilation of CO2 in the two hydrothermal vent animals, the mussel *Bathymodiolus thermophilus* and the tubeworm *Riftia pachyptila*. *The Biological Bulletin* 170(1):110–121.
12. Nelson DC, Hagen KD, Edwards DB (1995) The gill symbiont of the hydrothermal vent mussel *Bathymodiolus thermophilus* is a psychrophilic, chemoautotrophic, sulfur bacterium. *Marine Biology* 121(3):487–495.
13. Dubilier N, Bergin C, Lott C (2008) Symbiotic diversity in marine animals: The art of harnessing chemosynthesis. *Nat Rev Microbiol* 6(10):725–740.
14. Ramirez-Llodra E, Shank TM, German CR (2007) Biodiversity and biogeography of hydrothermal vent species thirty years of discovery and investigations. *Oceanography (Washington DC)* 20(1):30–41.
15. Butterfield DA, et al. (1994) Gradients in the composition of hydrothermal fluids from the Endeavour segment vent field: Phase separation and brine loss. *Journal of Geophysical Research* 99(B5):9561–9583.
16. Butterfield DA, Massoth GJ, McDuff RE, Lupton JE, Lilley MD (1990) Geochemistry of hydrothermal fluids from axial seamount hydrothermal emissions study vent field, Juan-de-Fuca Ridge - subseafloor boiling and subsequent fluid-rock interaction. *Journal of Geophysical Research-Solid Earth and Planets* 95(B8):12895–12921.
17. Von Damm KL (1995) Controls on the chemistry and temporal variability of seafloor hydrothermal fluids. *Seafloor Hydrothermal Systems: Physical, Chemical, Biological, and Geological Interactions,* Geophys Monogr Ser (American Geophysical Union, Washington, DC), 91:222–247.
18. Tivey MK (2007) Generation of seafloor hydrothermal vent fluids and associated mineral deposits. *Oceanography (Washington DC)* 20(1):50–65.
19. Shank TM, et al. (1998) Temporal and spatial patterns of biological community development at nascent deep-sea hydrothermal vents (9°50'N, East Pacific Rise). *Deep Sea Research Part II: Topical Studies in Oceanography* 45(1–3):465–515.
20. Hessler RR, et al. (1988) Temporal change in megafauna at the Rose Garden hydrothermal vent (Galapagos Rift; eastern tropical Pacific). *Deep Sea Research Part A: Oceanographic Research Papers* 35(10–11):1681–1709.
21. Fisher CR, et al. (1988) Microhabitat variation in the hydrothermal vent mussel, *Bathymodiolus thermophilus*, at the Rose Garden vent on the Galapagos Rift. *Deep Sea Research Part A: Oceanographic Research Papers* 35(10–11):1769–1791.
22. Waite TJ, et al. (2008) Variation in sulfur speciation with shellfish presence at a Lau Basin diffuse flow vent site. *Journal of Shellfish Research* 27(1):163–168.
23. Luther GW, 3rd, et al. (2001) Chemical speciation drives hydrothermal vent ecology. *Nature* 410(6830):813–816.
24. Moore TS, Shank TM, Nuzzio DB, Luther GW III (2009) Time-series chemical and temperature habitat characterization of diffuse flow hydrothermal sites at 9°50'N East Pacific Rise. *Deep Sea Research Part II: Topical Studies in Oceanography* 56(19–20): 1616–1621.
25. Fisher CR, et al. (1988) Variation in the hydrothermal vent clam, *Calyptogena magnifica*, at the Rose Garden vent on the Galapagos spreading center. *Deep Sea Research Part A: Oceanographic Research Papers* 35(10-11):1811–1831.
26. Le Bris N, Govenar B, Le Gall C, Fisher CR (2006) Variability of physico-chemical conditions in 9°50'N EPR diffuse flow vent habitats. *Marine Chemistry* 98(2–4):167–182.
27. Le Bris N, Sarradin PM, Caprais JC (2003) Contrasted sulphide chemistries in the environment of 13°N EPR vent fauna. *Deep Sea Research Part I: Oceanographic Research Papers* 50(6):737–747.
28. Podowski EL, Ma S, Luther GW III, Wardrop D, Fisher CR (2010) Biotic and abiotic factors affecting distributions of megafauna in diffuse flow on andesite and basalt along the Eastern Lau Spreading Center, Tonga. *Marine Ecology Progress Series* 418: 25–45.
29. Podowski EL, Moore TS, Zelnio KA, Luther GW, Fisher CR (2009) Distribution of diffuse flow megafauna in two sites on the Eastern Lau Spreading Center, Tonga. *Deep-Sea Research Part I: Oceanographic Research Papers* 56(11):2041–2056.
30. Girguis PR, Childress JJ (2006) Metabolite uptake, stoichiometry and chemoautotrophic function of the hydrothermal vent tubeworm *Riftia pachyptila*: Responses to environmental variations in substrate concentrations and temperature. *Journal of Experimental Biology* 209(Pt 18):3516–3528.
31. Cavanaugh CM, McKiness ZP, Newton ILG, Stewart FJ (2007) Marine Chemosynthetic Symbioses. *The Prokaryotes*, eds Dworkin M, Falkow S, Rosenberg E, Schleifer K-H, Stackebrandt E (Springer, New York), pp 475–507.
32. Petersen JM, et al. (2011) Hydrogen is an energy source for hydrothermal vent symbioses. *Nature* 476(7359):176–180.
33. Kleiner M, et al. (2012) Metaproteomics of a gutless marine worm and its symbiotic microbial community reveal unusual pathways for carbon and energy use. *Proc Natl Acad Sci* 109(19):E1173–E1182.
34. Denis F, Jollivet D, Moraga D (1993) Genetic separation of two allopatric populations of hydrothermal snails *Alviniconcha* spp (Gastropoda) from two south western pacific back-arc basins. *Biochemical Systematics and Ecology* 21(4):431–440.
35. Kojima S, et al. (2001) Phylogeny of hydrothermal-vent-endemic gastropods *Alviniconcha* spp. from the western Pacific revealed by mitochondrial DNA sequences. *The Biological Bulletin* 200(3):298–304.
36. Suzuki Y, et al. (2005) Novel chemoautotrophic endosymbiosis between a member of the Epsilonproteobacteria and the hydrothermal-vent gastropod *Alviniconcha* aff. *hessleri* (Gastropoda: Provannidae) from the Indian Ocean. *Appl Environ Microbiol* 71 (9):5440–5450.
37. Suzuki Y, et al. (2005) Molecular phylogenetic and isotopic evidence of two lineages of chemoautotrophic endosymbionts distinct at the subdivision level harbored in one

host-animal type: The genus *Alviniconcha* (Gastropoda: Provannidae). *FEMS Microbiol Lett* 249(1):105–112.

38. Suzuki Y, et al. (2006) Host-symbiont relationships in hydrothermal vent gastropods of the genus *Alviniconcha* from the Southwest Pacific. *Appl Environ Microbiol* 72(2): 1388–1393.

39. Stein JL, et al. (1988) Chemoautotrophic symbiosis in a hydrothermal vent gastropod. *The Biological Bulletin* 174(3):373–378.

40. Urakawa H, et al. (2005) Hydrothermal vent gastropods from the same family (Provannidae) harbour epsilon- and gamma-proteobacterial endosymbionts. *Environ Microbiol* 7(5):750–754.

41. Martinez F, Taylor B, Baker ET, Resing JA, Walker SL (2006) Opposing trends in crustal thickness and spreading rate along the back-arc Eastern Lau Spreading Center: Implications for controls on ridge morphology, faulting, and hydrothermal activity. *Earth and Planetary Science Letters* 245(3–4):655–672.

42. Bézos A, Escrig S, Langmuir CH, Michael PJ, Asimow PD (2009) Origins of chemical diversity of back-arc basin basalts: A segment-scale study of the Eastern Lau Spreading Center. *Journal of Geophysical Research* 114(B6):B06212.

43. Escrig S, Bézos A, Goldstein SL, Langmuir CH, Michael PJ (2009) Mantle source variations beneath the Eastern Lau Spreading Center and the nature of subduction components in the Lau basin-Tonga arc system. *Geochemistry Geophysics Geosystems* 10(4):Q04014.

44. Mottl MJ, et al. (2011) Chemistry of hot springs along the Eastern Lau Spreading Center. *Geochimica Et Cosmochimica Acta* 75:1013–1038.

45. Hsu-Kim H, Mullaugh KM, Tsang JJ, Yucel M, Luther GW, 3rd (2008) Formation of Zn- and Fe-sulfides near hydrothermal vents at the Eastern Lau Spreading Center: Implications for sulfide bioavailability to chemoautotrophs. *Geochem Trans* 9(1):6.

46. Distel DL, Lee HK, Cavanaugh CM (1995) Intracellular coexistence of methano- and thioautotrophic bacteria in a hydrothermal vent mussel. *Proc Natl Acad Sci USA* 92(21):9598–9602.

47. Duperron S, et al. (2006) A dual symbiosis shared by two mussel species, *Bathymodiolus azoricus* and *Bathymodiolus puteoserpentis* (Bivalvia: Mytilidae), from hydrothermal vents along the northern Mid-Atlantic Ridge. *Environ Microbiol* 8(8): 1441–1447.

48. DeChaine EG, Cavanaugh CM (2006) Symbioses of Methanotrophs and Deep-Sea Mussels (Mytilidae: Bathymodiolinae). Molecular Basis of Symbiosis. *Progress in Molecular and Subcellular Biology*, ed Overmann J (Springer, Berlin), 41:227–249.

49. Endow K, Ohta S (1989) The symbiotic relationship between bacteria and a mesogastropod snail, *Alviniconcha hessleri,* collected from hydrothermal vents of the Mariana back-arc basin. *Bulletin of the Japanese Society of Microbial Ecology* 3(2): 73–82.

50. Vrijenhoek RC (2010) Genetic diversity and connectivity of deep-sea hydrothermal vent metapopulations. *Mol Ecol* 19(20):4391–4411.

51. Cowen RK, Sponaugle S (2009) Larval dispersal and marine population connectivity. *Annu Rev Mar Sci* 1(1):443–466.

52. Waren A, Bouchet P (1993) New records, species, genera, and a new family of gastropods from hydrothermal vents and hydrocarbon seeps. *Zoologica Scripta* 22(1):1–90.

53. Speer K, Thurnherr AM (2012) The Lau Basin float experiment (LAUB-FLEX). *Oceanography (Washington DC)* 25(1):284–285.

54. Martinez F, Taylor B (2002) Mantle wedge control on back-arc crustal accretion. *Nature* 416(6879):417–420.

55. Taylor B, Martinez F (2003) Back-arc basin basalt systematics. *Earth and Planetary Science Letters* 210(3-4):481–497.

56. Dunn RA, Martinez F (2011) Contrasting crustal production and rapid mantle transitions beneath back-arc ridges. *Nature* 469(7329):198–202.

57. Proskurowski G, Lilley MD, Olson EJ (2008) Stable isotopic evidence in support of active microbial methane cycling in low-temperature diffuse flow vents at 9°50'N East Pacific Rise. *Geochimica Et Cosmochimica Acta* 72(8):2005–2023.

58. Butterfield DA, Massoth GJ (1994) Geochemistry of north Cleft segment vent fluids: Temporal changes in chlorinity and their possible relation to recent volcanism. *Journal of Geophysical Research* 99(B3):4951–4968.

59. Butterfield DA, et al. (1997) Seafloor eruptions and evolution of hydrothermal fluid chemistry. *Philosophical Transactions of the Royal Society of London. Series A: Mathematical, Physical and Engineering Sciences* 355(1723):369–386.

60. Yamamoto M, Takai K (2011) Sulfur metabolisms in epsilon- and gamma-Proteobacteria in deep-sea hydrothermal fields. *Frontiers in Microbiology*, 10.3389/fmicb.2011.00192.

61. Nakagawa S, Takai K (2008) Deep-sea vent chemoautotrophs: Diversity, biochemistry and ecological significance. *FEMS Microbiol Ecol* 65(1):1–14.

62. Macalady JL, et al. (2008) Niche differentiation among sulfur-oxidizing bacterial populations in cave waters. *ISME J* 2(6):590–601.

63. Campbell BJ, Engel AS, Porter ML, Takai K (2006) The versatile epsilon-proteobacteria: Key players in sulphidic habitats. *Nat Rev Microbiol* 4(6):458–468.

64. Nakagawa S, et al. (2005) Distribution, phylogenetic diversity and physiological characteristics of epsilon-Proteobacteria in a deep-sea hydrothermal field. *Environ Microbiol* 7(10):1619–1632.

65. Nakagawa S, Takaki Y (2001) *Nonpathogenic Epsilonproteobacteria* (John Wiley and Sons, Ltd, Chichester). Available at http://www.els.net.

66. Henry MS, Childress JJ, Figueroa D (2008) Metabolic rates and thermal tolerances of chemoautotrophic symbioses from Lau Basin hydrothermal vents and their implications for species distributions. *Deep-Sea Research Part I: Oceanographic Research Papers* 55(5):679–695.

67. Wittenberg JB, Stein JL (1995) Hemoglobin in the symbiont-harboring gill of the marine gastropod Alviniconcha hessleri. *The Biological Bulletin* 188(1):5–7.

68. Matabos M, Le Bris N, Pendlebury S, Thiebaut E (2008) Role of physico-chemical environment on gastropod assemblages at hydrothermal vents on the East Pacific Rise (13°N/EPR). *Journal of the Marine Biological Association of the United Kingdom* 88(05):995–1008.

69. Thornhill DJ, Kemp DW, Bruns BU, Fitt WK, Schmidt GW (2008) Correspondence between cold tolerance and temperatre biogeography in a western Atlantic *Symbiodinium* (Dinophyta) lineage. *Journal of Phycology* 44(5):1126–1135.

70. Verde E, McCloskey L (2007) A comparative analysis of the photobiology of zooxanthellae and zoochlorellae symbiotic with the temperate clonal anemone *Anthopleura elegantissima* (Brandt). III. Seasonal effects of natural light and temperature on photosynthesis and respiration. *Marine Biology* 152(4):775–792.

71. Iglesias-Prieto R, Beltrán VH, LaJeunesse TC, Reyes-Bonilla H, Thomé PE (2004) Different algal symbionts explain the vertical distribution of dominant reef corals in the eastern Pacific. *Proc Biol Sci* 271(1549):1757–1763.

72. Loram JE, Trapido-Rosenthal HG, Douglas AE (2007) Functional significance of genetically different symbiotic algae Symbiodinium in a coral reef symbiosis. *Mol Ecol* 16(22):4849–4857.

73. Bongaerts P, et al. (2010) Genetic divergence across habitats in the widespread coral *Seriatopora hystrix* and its associated *Symbiodinium. PLoS ONE* 5(5):e10871.

74. Finney JC, et al. (2010) The relative significance of host-habitat, depth, and geography on the ecology, endemism, and speciation of coral endosymbionts in the genus Symbiodinium. *Microb Ecol* 60(1):250–263.

75. Ferrari J, et al. (2004) Linking the bacterial community in pea aphids with host-plant use and natural enemy resistance. *Ecol Entomol* 29(1):60–65.

76. Ferrari J, Scarborough CL, Godfray HC (2007) Genetic variation in the effect of a facultative symbiont on host-plant use by pea aphids. *Oecologia* 153(2):323–329.

77. Tsuchida T, Koga R, Shibao H, Matsumoto T, Fukatsu T (2002) Diversity and geographic distribution of secondary endosymbiotic bacteria in natural populations of the pea aphid, *Acyrthosiphon pisum. Mol Ecol* 11(10):2123–2135.

78. Halary S, Riou V, Gaill F, Boudier T, Duperron S (2008) 3D FISH for the quantification of methane- and sulphur-oxidizing endosymbionts in bacteriocytes of the hydrothermal vent mussel *Bathymodiolus azoricus. ISME J* 2(3):284–292.

79. Riou V, et al. (2008) Influence of CH_4 and H_2S availability on symbiont distribution, carbon assimilation and transfer in the dual symbiotic vent mussel *Bathymodiolus azoricus. Biogeosciences* 5(6):1681–1691.

80. Fujiwara Y, et al. (2000) Phylogenetic characterization of endosymbionts in three hydrothermal vent mussels: Influence on host distributions. *Marine Ecology Progress Series* 208:147–155.

81. Van Dover CL (2002) Community structure of mussel beds at deep-sea hydrothermal vents. *Marine Ecology Progress Series* 230:137–158.

82. Cordes EE, Becker EL, Hourdez S, Fisher CR (2010) Influence of foundation species, depth, and location on diversity and community composition at Gulf of Mexico lower-slope cold seeps. *Deep Sea Research Part II: Topical Studies in Oceanography* 57(21–23):1870–1881.

83. Luther GW III, et al. (2008) Use of voltammetric solid-state (micro)electrodes for studying biogeochemical processes: Laboratory measurements to real time measurements with an in situ electrochemical analyzer (ISEA). *Marine Chemistry* 108(3–4):221–235.

84. Gartman A, et al. (2011) Sulfide oxidation across diffuse flow zones of hydrothermal vents. *Aquatic Geochemistry* 17(4):583–601.

85. Seewald JS, Doherty KW, Hammar TR, Liberatore SP (2002) A new gas-tight isobaric sampler for hydrothermal fluids. *Deep Sea Research Part I: Oceanographic Research Papers* 49(1):189–196.

86. Shapiro B, Rambaut A, Drummond AJ (2006) Choosing appropriate substitution models for the phylogenetic analysis of protein-coding sequences. *Mol Biol Evol* 23(1): 7–9.

87. Drummond AJ, Rambaut A (2007) BEAST: Bayesian evolutionary analysis by sampling trees. *Australian Journal of Ecology* 7(1):214.

88. Clarke KR (1993) Non-parametric multivariate analyses of changes in community structure. *Australian Journal of Ecology* 18(1):117–143.